J Toxicol Pathol 2013; 26: 275–281

Original Article

Corneal Mineralization in Wistar Hannover Rats

Satomi Hashimoto[1], Takuya Doi[1], Yumi Wako[1], Junko Sato[1], Sou Wada[2], and Minoru Tsuchitani[1*]

[1] Pathology Department, Kashima Laboratory, Nonclinical Research Center, Mitsubishi Chemical Medience Corporation, 14-1 Sunayama, Kamisu, Ibaraki 314-0255, Japan
[2] Safety Assessment Department, Kashima Laboratory, Nonclinical Research Center, Mitsubishi Chemical Medience Corporation, 14-1 Sunayama, Kamisu, Ibaraki 314-0255, Japan

Abstract: We have recently started using Wistar Hannover rats in Japan and are now collecting background data. We have been frequently observing corneal mineralization in Wistar Hannover rats of both the RccHan^{TM}:WIST and Crl:WI (Han) strains. In this study, details of corneal mineralization in Wistar Hannover rats were histopathologically and ultrastructurally investigated. According to the results, Wistar Hannover rats had a much higher incidence of corneal mineralization compared with Sprague-Dawley rats. The incidence of corneal mineralization was higher in males than females. According to the histological examination, mineral deposits were positive for calcium by von Kossa's method. Furthermore, in response to mineralization, keratocytes probably become active to play an important role against the mineralized substance. (DOI: 10.1293/tox.26.275; J Toxicol Pathol 2013; 26: 275–281)

Key words: Wistar Hannover rat, Background data, Cornea, Mineralization, Keratocyte

Introduction

Corneal mineralization occurs along the basement membrane or in the subepithelial stroma in both humans and animals and is observed as a basophilic deposit in sections stained with hematoxylin and eosin (HE)[1]. Ultrastructurally, the deposit is composed of aggregating spherules and amorphous material and occasionally shows a laminar appearance[2–4]. X-ray microanalysis reveals that the deposit predominantly consists of calcium and phosphorus[2,5,6].

In humans, corneal mineralization is known as calcific band keratopathy and is thought to be associated with the morbid systemic condition that leads to an increase in serum calcium levels such as hyperparathyroidism, hypocalcemia of malignancy and excessive vitamin D therapy[1]. There are various factors thought to be responsible for the pathogenesis of calcific band keratopathy, such as localized damage and dryness of the cornea[4].

In rodents, spontaneous corneal mineralization has been reported in Fischer 344, Sprague-Dawley (SD) and Wistar rats and CD-1, CF_1, C3H, DBA/2, $CD2F_1$ and BALB/c mice but not in Lewis rats[1,3,6–9]. In mice, mineralization with or without corneal edema, ulcer, erosion or vascularization is sometimes observed[10] and is thought to be related to the frequency of cage cleaning and the ammonia levels in the cage[9]. In rats, although details of its pathogenesis are not clear, it is thought to be a primary change because mineralization is observed without epithelial defects or inflammatory reactions[3,6].

At present, there are a still few studies using Wistar Hannover rats in Japan; therefore, we are collecting background data. Through this work, we realized that there were high incidences of corneal mineralization in Wistar Hannover rats. A greater incidence of corneal mineralization in Wistar Hannover rats as one of the histological characteristics of this strain was reported[11], but to our knowledge, there are no reports concerning histological details of corneal mineralization in this strain. In this study, we demonstrated the histopathological and ultrastructural characteristics of corneal mineralization in Wistar Hannover rats, as well as its incidence.

Materials and Methods

Animals

We used the eyes of Wistar Hannover rats (720 animals) from two providers and SD rats (102 animals) for comparison. RccHan^{TM}:WIST (Rcc) rats (240 males and 240 females) from Japan Laboratory Animals, Inc. (Saitama, Japan) and Crl:WI (Han) (Crl) rats (120 males and 120 females) from Charles River Laboratories Japan, Inc. (Shiga, Japan) were obtained at 4 weeks of age. They were housed

Received: 8 January 2013, Accepted: 18 March 2013
*Corresponding author: M Tsuchitani (e-mail: Tsuchitani.Minoru@mp.medience.co.jp)

individually in hanging-type stainless steel wire mesh cages (195W × 325D × 180H mm, Tokiwa Kagaku Kikai Co., Ltd., Tokyo, Japan) in an animal room maintained at 22 ± 3°C with a relative humidity of 55 ± 20%, air ventilation 6 to 20 times per hour and a 12-hour light/dark cycle. The room was cleaned every day, and the sanitary trays containing hardwood chips placed under the cages were replaced at least once a week. The ammonia levels in the room were kept below 4 ppm. Pelleted diet (radiation sterilized CR-LPF, Oriental Yeast Co., Ltd., Tokyo, Japan) and drinking water (tap water, via automatic water supply system) were provided *ad libitum*. Animals were divided into four groups for euthanasia at 8, 10, 19 and 32 weeks of age for Rcc rats and into two groups at 19 and 32 weeks of age for Crl rats, with each group consisting of 60 animals of each sex (Tables 1 and 2). Each group was derived from two different lots, with each lot consisting of 30 animals of each sex (data not shown). Additionally, 2 female Rcc rats at 110 weeks were necropsied, and their eyes were subjected to a histological examination in order to demonstrate the presence of calcium; the eyes of 3 male Rcc rats at 14 weeks were examined ultrastructurally. The eyes of 102 SD rats (Charles River Laboratories Japan, Inc., Ibaraki, Japan) consisted of eyes from 51 males and 51 females at 9 to 15 weeks of age derived from control

Table 1. Number of Animals and Incidence of Corneal Mineralization (%) in RccHan^{TM}:WIST Rats

		Rcc[1)]								
	Week of age	Number of animals examined	Number of animals with mineralization					Number of animals with activated keratocytes[2)]	Number of animals with mineralization and/or activated keratocytes	
			Form			Total	Incidence %		Total	Incidence %
			Granular	Linear	Coarse					
Male	8	60	10 (7)	4 (4)	0 (0)	14	23.3	8	22	36.7
	10	60	13 (7)	17 (13)	5 (5)	23[3)]	38.3	6	29	48.3
	19	60	8 (4)	20 (17)	11 (11)	21	35.0	2	23	38.3
	32	60	9 (2)	24 (14)	6 (4)	24[4)]	40.0	0	24	40.0
Female	8	60	7 (2)	4 (2)	0 (0)	10	16.7	5	15	25.0
	10	60	6 (3)	11 (9)	4 (4)	12[5)]	20.0	7	19	31.7
	19	60	4 (1)	14 (12)	7 (6)	14	23.3	0	14	23.3
	32	60	4 (0)	13 (5)	6 (4)	16[6)]	26.7	0	16	26.7
Total		480				134		28	162	

1) Rcc, RccHan^{TM}: WIST derived from Japan Laboratory Animals, Inc. 2) Number of animals with no visible mineral deposits but activated keratocytes. 3) This is composed of 11 out of 30 rats subjected to ophthalmoscopy and 12 out of 30 rats that were not. 4) This is composed of 13 out of 30 rats subjected to ophthalmoscopy and 11 out of 30 rats that were not. 5) This is composed of 3 out of 30 rats subjected to ophthalmoscopy and 9 out of 30 rats that were not. 6) This is composed of 10 out of 30 rats subjected to ophthalmoscopy and 6 out of 30 rats that were not. The number of animals with both mineral deposits and activated keratocytes is shown in parentheses.

Table 2. Number of Animals and Incidence of Corneal Mineralization (%) in Crl:WI (Han) Rats

		Crl[1)]								
	Week of age	Number of animals examined	Number of animals with mineralization					Number of animals with activated keratocytes[2)]	Number of animals with mineralization and/or activated keratocytes	
			Form			Total	Incidence %		Total	Incidence %
			Granular	Linear	Coarse					
Male	8	-	-	-	-	-	-	-	-	-
	10	-	-	-	-	-	-	-	-	-
	19	60	9 (2)	27 (20)	9 (9)	28	46.7	0	28	46.7
	32	60	22 (2)	39 (19)	12 (9)	41[3)]	68.3	0	41	68.3
Female	8	-	-	-	-	-	-	-	-	-
	10	-	-	-	-	-	-	-	-	-
	19	60	2 (0)	11 (5)	4 (3)	13	21.7	0	13	21.7
	32	60	17 (3)	21 (9)	6 (5)	24[4)]	40.0	0	24	40.0
Total		240				106		0	106	

1) Crl, Crl:WI (Han) derived from Charles River Laboratories Japan, Inc. 2) Number of animals with no visible mineral deposits but activated keratocytes. 3) This is composed of 20 out of 30 rats subjected to ophthalmoscopy and 21 out of 30 rats that were not. 4) This is composed of 15 out of 30 rats subjected to ophthalmoscopy and 9 out of 30 rats that were not. The number of animals with both mineral deposits and activated keratocytes is shown in parentheses. -, Not examined.

groups of toxicity studies conducted in our laboratory from 2009 to 2010, and these were examined retrospectively for comparison. Half of the Rcc rats of both sexes sacrificed at 10 weeks of age were used for the ophthalmoscopic examinations three times, at 5, 7 and 9 weeks of age, and half of the Rcc and Crl rats of both sexes sacrificed at 32 weeks of age were used for ophthalmoscopic examinations four times, at 5, 9, 18 and 31 weeks of age. Moreover, all 102 SD rats derived from control groups in the toxicity studies experienced ophthalmoscopic examinations twice. The animals were cared for according to the principles outlined in the guides for the care and use of laboratory animals prepared by the Japanese Association for Laboratory Animal Science and our institution.

Histopathological examination

For the histopathological examination, the animals were anesthetized with an intraperitoneal injection of sodium thiopental (Ravonal®, Mitsubishi Tanabe Pharma Corporation, Osaka, Japan) and euthanized by exsanguination from the abdominal aorta. Then, the eyes and other organs/tissues were removed. The eyes of 720 Wistar Hannover rats, including both Rcc and Crl rats, were fixed in Davidson's solution and subsequently trimmed and fixed in 10% phosphate-buffered formalin solution. The fixed eyes were embedded in paraffin, cut at a thickness of 5 μm and stained with HE. All eyes were examined using a light microscope. The eyes of 2 additional Rcc rats were fixed in 10% phosphate-buffered formalin solution to demonstrate the presence of calcium by von Kossa's method. The sections of these additional eyes stained by von Kossa's method or with HE were also examined using a light microscope.

Ultrastructural examination

For the electron microscopical examination, the eyes of the 3 Rcc rats described above were fixed in 10% neutral buffed formalin solution for the first fixation. Then, the corneas were cut out from the eyes, divided in quarters, postfixed in 1% osmium tetroxide, and embedded in epoxy resin. Ultrathin sections were stained with uranyl acetate and lead citrate, and observed under an electron microscope (H-7600, Hitachi, Tokyo, Japan).

Results

Incidence of corneal mineralization

In SD rats, no corneal mineralization was observed in either sex (data not shown). On the other hand, in Wistar Hannover rats, there was a high incidence of corneal mineralization as shown in Table 1 and Table 2. At 8,10,19 and 32 weeks, the incidences of mineralization in Rcc rats were 23.3, 38.3, 35.0 and 40.0% in males and 16.7, 20.0, 23.3 and 26.7% in females, respectively. Furthermore, those at 19 and 32 weeks in Crl rats were 46.7 and 68.3% in males and 21.7 and 40.0% in females, respectively. In both Rcc and Crl rats, males showed a higher incidence of corneal mineralization than females. The incidences of mineralization in Wistar Hannover rats did not differ whether the ophthalmoscopic examinations were performed or not (details of the number of animals with mineralization are shown in the footnotes of Tables 1 and 2).

Histopathological findings

Corneal mineralization was located in the center of the cornea but was not observed in the corneal limbus. Various forms of corneal mineralization such as basophilic granular (Fig. 1A), linear (Fig. 1B, C) or coarse deposits (Fig. 1D, E) were observed with HE staining in a total of 134 Rcc and 106 Crl rats representing every age group (Tables 1 and 2). Deposits were observed along the basement membrane of the corneal epithelium, on the anteriormost part of the corneal stroma (Fig. 1A, B, D, E) or within the stroma at a short distance from the basement membrane (Fig. 1C). Deposits in the corneas fixed with 10% phosphate-buffered formalin solution were positive for calcium by von Kossa's method (Fig. 1G). Although keratocytes are normally thin and parallel the collagen laminae in the stroma, near the deposit, some cells with round to oval nuclei and prominent nucleoli were often observed (Fig. 1D), indicating that they were activated keratocytes. These activated keratocytes were also present between the corneal epithelium and the deposits (Fig. 1E). Furthermore, even if there were no visible basophilic deposits, we could often see some activated keratocytes in the anterior part of the stroma (Fig. 1F) in a total of 28 Rcc rats from the 8-, 10- and 19-week groups (Table 1). Occasionally, between the corneal epithelium and the stroma, distinct clefts accompanied the deposits or activated keratocytes (Fig. 1E, F).

The numbers of animals with mineralization of each form, including the 3 forms of mineral deposits and activated keratocytes with no visible deposits, are shown in Tables 1 and 2. In Rcc rats at 8 weeks, most of the mineral deposits were of the granular form, and no deposits with the coarse form were observed. In Rcc rats at more than 10 weeks, there were 3 deposit forms, and an increase in the incidence of the coarse deposit form with aging was not observed. In both Rcc and Crl rats, activated keratocytes tended to be observed more frequently nearer coarse deposits rather than nearer granular and linear deposits. In Rcc and Crl rats at 19 and 32 weeks, activated keratocytes without any visible deposits were not observed, except in the case of 2 male Rcc rats at 19 weeks. This was observed mainly in younger rats at 8 and 10 weeks.

Ultrastructural findings

The electron microscopic examination revealed details of the granular (Fig. 2A), linear (Fig. 2B, C) and coarse forms (Fig. 2D) of the mineral deposits. The deposits were composed of aggregating spherules and amorphous materials, which often made laminated high and low electron dense plaques (Fig. 2A, C, D). The laminae were roughly parallel to the outermost contour of each deposit. In all forms, although the epithelial basal cells overlying the deposit formed irregular basal invaginations, their basement

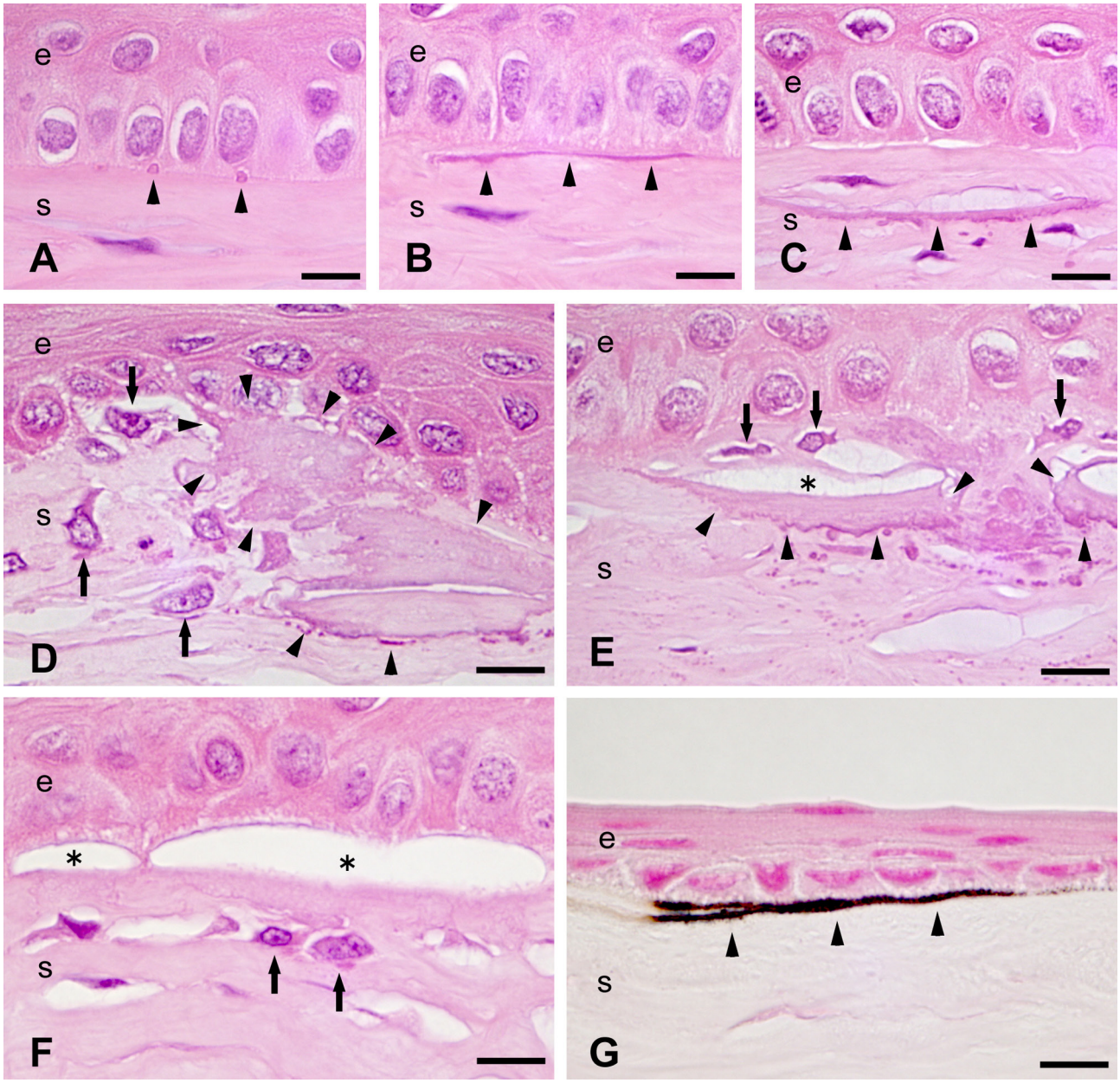

Fig. 1. Cornea with various forms of mineralization in Wistar Hannover rats. A, B, C: Granular (A) and linear (B, C) deposits (arrowheads) in 32-week-old male Crl rats. HE. They occurred along the basement membrane of the corneal epithelium, on the anterior edge of the corneal stroma (A, B) or within the stroma at some distance away from the edge (C). D, E: Coarse deposits (arrowheads) in 32-week-old male Rcc rats. HE. Near the deposits, some activated keratocytes with round to oval nuclei and prominent nucleoli can be observed (arrows). Among these, three keratocytes between the corneal epithelium and deposits can be observed (E, arrows). Near the deposits or activated keratocytes, there is occasionally a distinct cleft below the corneal epithelium (E, asterisk). F: Two activated keratocytes (arrows) and clefts (asterisks) without any visible mineral deposits in a 10-week-old male Rcc rat. HE. G: Linear deposit (arrowheads) in a 110-week-old female Rcc rat. Von Kossa's method. The deposit is positive for calcium. e, corneal epithelium; s, corneal stroma. Bar = 10 μm.

membranes were on the epithelial side and did not peel off (Fig. 2A–D), and there were hemidesmosomes in epithelial cells facing the basement membrane (Fig. 2E, F), indicating that each epithelial cell itself was intact. Based on this, every deposit existed mainly in the anterior part of the corneal stroma just below the epithelial basement membrane or sometimes in the stroma at some distance away from the basement membrane (Fig. 1C). Activated keratocytes that were slightly expanded and extending their cytoplasmic processes were observed near deposits (Fig. 2C, D). Some of them were between deposits and the epithelium, with fine collagen fibrils around them (Fig. 2G, H).

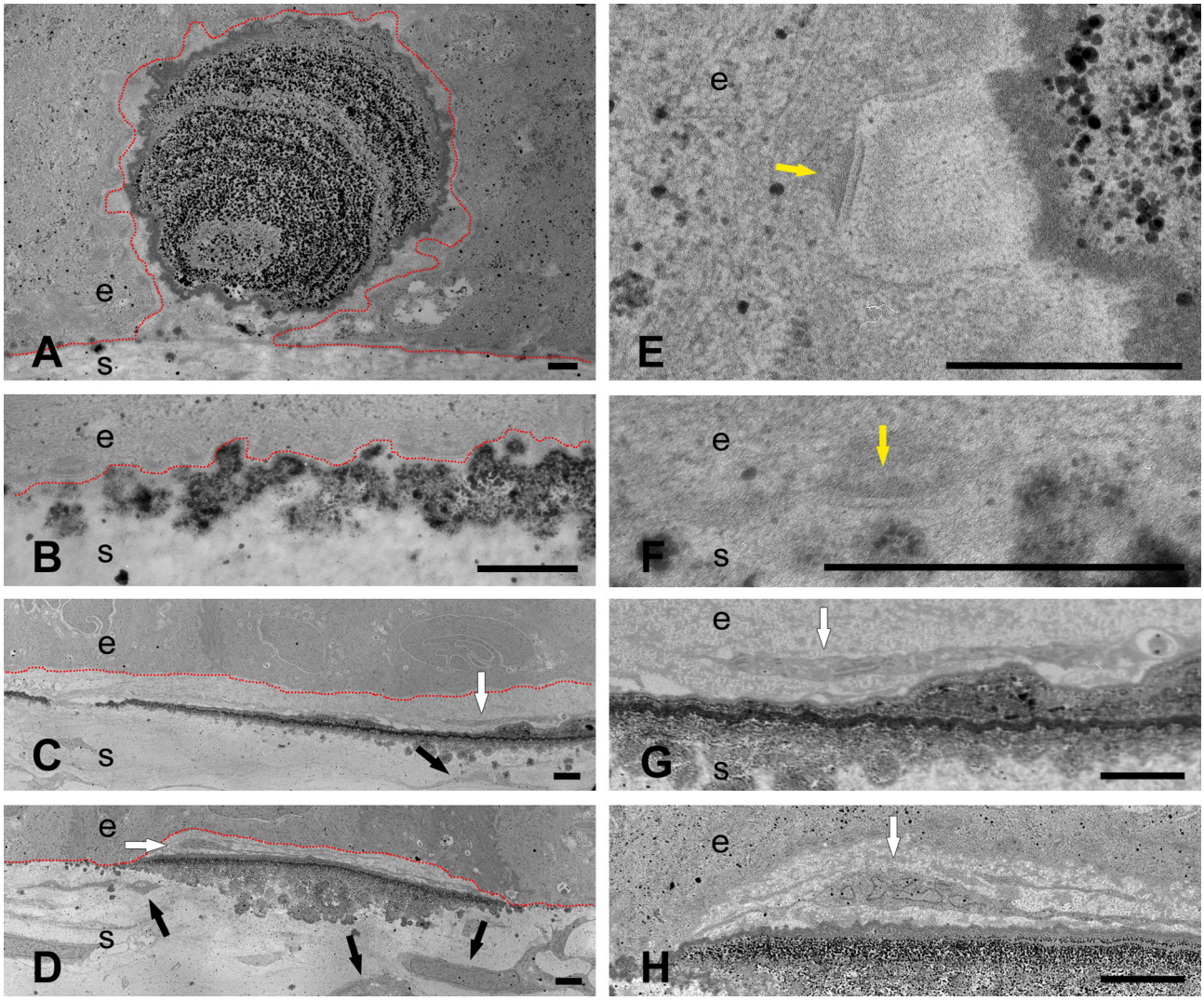

Fig. 2. Electron micrographs of various forms of corneal mineralization in a 14-week-old male Rcc rat. A–D: Granular (A), linear (B, C) and coarse (D) deposits can be observed in the anterior part of the corneal stroma just below the epithelial basement membrane (red dashed lines) or inside the stroma at some distance away from the basement membrane (C). Each deposit is composed of aggregating spherules and amorphous materials, and they often produce laminated high and low electron dense plaques (A, C, D). Activated keratocytes (arrows) are observed near the deposits (C, D). Furthermore, some are between the epithelium and the deposits (C, D, white arrows). E, F: Higher magnification of A and B. There are hemidesmosomes (yellow arrows) in the epithelial cell facing the basement membrane. G, H: Higher magnification of C and D. Fine collagen fibrils are observed around activated keratocytes (white arrows). e, corneal epithelium; s, corneal stroma. Bar =0.5 µm (A, B, E, F) and 2.0 µm (C, D, G, H).

Discussion

The incidence of mineralization was higher in Wistar Hannover rats than SD rats, and the interstrain variation suggests a close relation with the genetic factor[1]. In both Rcc and Crl, the incidence of mineralization was higher in male rats. An association with the testosterone concentration in male SD rats has been previously reported[7]. We often observed activated keratocytes in the corneal stroma near mineral deposits. Furthermore, without any clear basophilic deposits, we observed some activated keratocytes in the anterior part of the stroma in 28 Rcc rats. As there were no other histological or ultrastructural abnormalities in the corneas, we surmised that the activation of keratocytes must be attributed only to mineralization. In fact, in some corneas, no mineralization was observed histologically, but very fine deposits were observed ultrastructurally as described in a past report[3]. Therefore, we also counted the number of animals with no visible mineral deposits except for activated keratocytes as a kind of corneal mineralization, in addition to the number of animals with clearly observable mineral deposits.

In the histopathological examination, the 3 deposit forms of corneal mineralization were observed. At the youngest age (8 weeks), the most common form was the granular form, and the coarse deposit form was not ob-

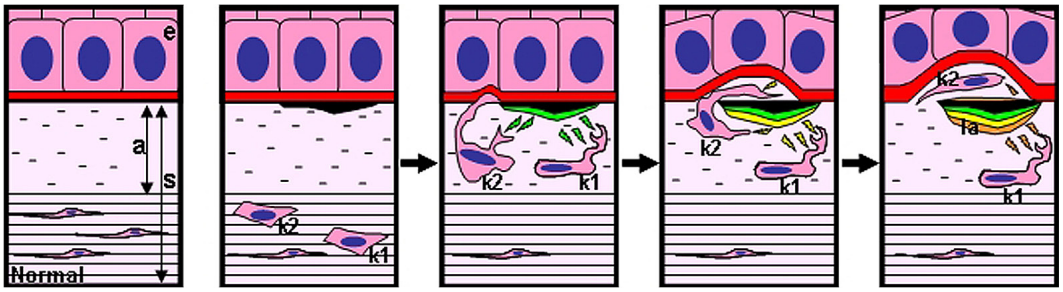

Fig. 3. This figure suggests the role of keratocytes with regard to mineral deposits. e, corneal epithelium; s, corneal stroma; a, the anterior part of the corneal stroma; k (k1, k2), keratocytes; la, laminated coarse mineral deposit.

served. However, at more than 10 weeks, all 3 mineral deposit forms were observed. Furthermore, mainly at younger ages (8 and 10 weeks), activated keratocytes without any visible deposits were observed. These findings suggest that at 8 and 10 weeks, the mineral deposits were too small to be recognized in the histopathological examination, but the keratocytes could notice this mineralization and be activated. Then, by 19 weeks, the small mineral deposits may have aggregated and formed granular, linear or coarse deposits.

In the histopathological examination, distinct clefts between the corneal epithelium and the stroma near deposits or activated keratocytes were observed. The cleft was reported to be an artifact in rats and mice[2,10]. Moreover, in calcific band keratopathy of humans, the anterior part of the corneal stroma, the so-called "Bowman's layer," often becomes detached from the underlying deposit because of its brittleness[4]. We consider that the cleft, especially that observed with mineralization or activated keratocytes, resulted from the weakening of adhesion in the anterior part of the corneal stroma.

In this study, the corneal mineral deposits in Wistar Hannover rats were positive for calcium by von Kossa's method, and the serum calcium level was normal (data not shown), as seen with other strains of rats[1,5,7]. Corneal stromal tissue contains calcium at a nearly saturated concentration, and even minor alterations in its microenvironment could induce an increase in pH or dryness and result in the precipitation of calcium[1–4,12,13]. The structure of the cornea of Wistar Hannover rats may be more susceptible to an increase in pH and dryness than that of SD rats. Besides, it is unlikely that ammonia is associated with the pathogenesis of corneal mineralization like mice because the frequency of air ventilation, room cleaning and sanitary tray replacement kept the ammonia level below 4 ppm, which is widely accepted as appropriate for animal housing conditions. Moreover, though half of the Wistar Hannover rats sacrificed at 10 and 32 weeks of age and all SD rats had 2–4 ophthalmological examinations in this study, it did not increase the incidence or size of mineralization (size data not shown).

Bellhorn *et al.* reported corneal mineralization without any other corneal lesions as spontaneous corneal degeneration in the rat and considered the calcific keratopathy in the rat to be spontaneous and possibly of a primary origin rather than degeneration secondary to other corneal disease[3]. On the other hand, corneal mineralization in mice was reported with other corneal lesions, such as necrosis and disorganization of the basal epithelium, corneal erosions and ulcers, neutrophils in the corneal stroma and thinning of the overlying epithelium[9]. So it is appropriate to consider that the mineralization occurred in relation to keratitis. Similarly, the mineralization of the coarse form in our rats possibly appeared as a healing feature of traumatic keratitis, though other corneal lesions were not observed except for activated keratocytes.

In this study, the mineralized deposits were present in the anterior part of the corneal stroma, mainly just below the epithelial basement membrane, and this was almost consistent with previous reports[1–4,6,7]. The anterior part of the corneal stroma is a special differentiated area of the corneal stroma and corresponds to the Bowman's layer in humans[15]. Small and sparse collagen fibrils are present there randomly[3,4,14] and may act as a nidus for or a filter against the precipitation at the beginning of mineralization[2–4]. We consider that the anterior part of the corneal stroma in Wistar Hannover rats is vulnerable to the precipitation of calcium.

Activated keratocytes were often observed near mineral deposits in the anterior part of the corneal stroma, where there are normally very few cellular components. They were recognized not only below mineral deposits but also between the deposits and the epithelium and were accompanied by fine collagen fibrils surrounding them. Keratocytes are fibroblasts in the corneal stroma[15]. When the cornea is damaged, it becomes active and produces collagen fibrils to repair and maintain the corneal tissue[6,10,16]. We surmised that keratocytes play a role against mineralization (Fig. 3). Keratocytes react to mineral deposits immediately, activating and locating near them, and produce collagen fibrils there. Activated keratocytes might infiltrate between the corneal epithelium and deposits (Fig. 3, k2) as well as below deposits (Fig. 3, k1) to separate the deposits from the corneal epithelium, because the anterior part of the corneal stroma (Fig. 3, a) corresponding to the Bowman's layer in humans lacks or contains very few keratocytes originally. In the histopathological observations, activated keratocytes

were more remarkable near coarse deposits than near granular and linear deposits. It has also been reported in mice that the collagen fibrils produced by activated keratocytes could be a new nidus for mineralizaition[10]. Therefore, in some cases, the more keratocytes producing fibrils, the larger the mineralized deposit becomes. This may have resulted in formation of the laminated coarse mineral deposits observed in the ultrastructural examination (Fig. 3, la).

In conclusion, we found that corneal mineralization frequently occurs in Wistar Hannover rats and at a higher incidence in males. The high incidence of mineralization is one of the characteristics of Wistar Hannover rats. Furthermore, keratocytes have a close relationship with corneal mineralization.

Acknowledgments: The authors would like to thank Japan Laboratory Animals, Inc. and Charles River Laboratories Japan, Inc. for providing the animals. We also thank Mr. Takayoshi Ito for his excellent technical assistance and Mr. Steve Yamakami and Ms. Kanae Tamatsukuri for language editing. All authors disclose that there are no conflicts of interest that could inappropriately influence the outcome of the present study.

References

1. Greaves P. Nervous system and special sense organs. Eye. Cornea. In: Histopathology of Preclinical Toxicity Studies, 3rd ed. P Greaves (ed). Elsevier, Amsterdam. 888–894. 2007.
2. Wojcinski ZW, Houston B, Gragtmans B, Rogers J, Piscopo I, and Baker K. A spontaneous corneal change in Juvenile Wistar rats. J Comp Path. **120**: 281–294. 1999. [Medline]
3. Bellhorn RW, Korte GE, and Abrutyn D. Spontaneous corneal degeneration in the rat. Lab Anim Sci. **38**: 46–50. 1988. [Medline]
4. O'Connor GR. Calcific band keratopathy. Trans Am Ophthalmol Soc. **70**: 58–81. 1972. [Medline]
5. Weisse I. Nervous system and special sense organs. Aging and ocular changes. Age-associated pathologic changes. Corneal dystrophy. In: Pathobiology of the Aging Rat, vol. 2. U Mohr, DL Dungworth, and CC Capen (eds). ILSI Press, Washington, D.C. 77–79. 1994.
6. Losco PE, and Troup CM. Corneal dystrophy in Fischer 344 rats. Lab Anim Sci. **38**: 702–710. 1988. [Medline]
7. Wegener A, and Jochims K. Clinical, histological and ultrastructural characteristics of a spontaneous corneal opacity in Sprague-Dawley rats. Ophthalmic Res. **26**: 296–303. 1994. [Medline]
8. Sheldon WG, and Greenman DL. Spontaneous lesions in control BALB/C female mice. J Environ Pathol Toxicol. **3**: 155–167. 1980. [Medline]
9. Van Winkle TJ, and Balk MW. Spontaneous corneal opacities in laboratory mice. Lab Anim Sci. **36**: 248–255. 1986. [Medline]
10. Frame SR, and Slone TW. Special senses: Eye. Nonneoplastic and neoplastic changes in the eye. Nonneoplastic lesions. Cornea. In: Pathobiology of the Aging Mouse, vol. 2. U Mohr, DL Dungworth, CC Capen, WW Carlton, JP Sundberg, and JM Ward (eds). ILSI Press, Washington, D.C. 98–99. 1996.
11. Okamura T, Suzuki S, Ogawa T, Kobayashi J, Kusuoka O, Hatayama K, Mochizuki M, Hoshiya T, Okazaki S, and Tamura K. Background data for general toxicology parameters in RccHan^{TM}:WIST rats at 8, 10, 19, weeks of age. J Toxicol Pathol. **24**: 195–205. 2011. [Medline]
12. Usui T, Hara M, Satoh H, Moriyama N, Kagaya H, Amano S, Oshika T, Ishii Y, Ibaraki N, Hara C, Kunimi M, Noiri E, Tsukamoto K, Inatomi J, Kawakami H, Endou H, Igarashi T, Goto A, Fujita T, Araie M, and Seki G. Molecular basis of ocular abnormalities associated with proximal renal tubular acidosis. J Clin Invest. **108**: 107–115. 2001. [Medline]
13. Fabian RJ, Bond JM, and Drobeck HP. Induced corneal opacities in the rat. Brit J Ophthal. **51**: 124–129. 1967. [Medline]
14. Yamamoto T. Sensory organ. Cornea. In: Fine Structure of Cells and Tissues, Electron microscopic Atlas, Volume IV, Supporting and Muscular Tissues, Sensory Organ, Nervous System. E Yamada, T Yamamoto, and K Hama (eds). Igaku-shoin, Tokyo. 68–73. 1968; (in Japanese).
15. Fujita H, and Fujita T. Sensory organ. Optic organ. Eye. Tunica fibrosa bulbi. Cornea. In: Textbook of Histology Part 2, 3rd ed. H Fujita, and T Fujita (eds). Igaku-shoin, Tokyo. 415–418. 1992; (in Japanese).
16. Hori I. Electron microscopic studies on the formation of the basal lamina of the regenerating epithelium in wound healing. Journal of the Jûzen Medical Society. **83**: 379–400. 1974; (in Japanese).